Load Tests on Thin Pretensioned Pavement Slabs

A. P. CHRISTENSEN and R. L. JANES
Respectively, Development Engineer and formerly Senior Development Engineer, Research and Development Laboratories, Portland Cement Association, Skokie, Illinois

An investigation of the load response of prestressed concrete pavement slabs is in progress at the PCA Research and Development Laboratories. The first published result of this investigation was a theoretical procedure for determining the magnitude and distribution of stresses and deflections in prestressed concrete pavements beyond conditions to which the elastic theory is applicable. The theoretical procedure is specifically applicable to a centrally loaded infinite slab supported by a "dense liquid" foundation and prestressed equally in longitudinal and transverse directions.

To test the validity of the assumptions made in the analysis and to compare theoretical and measured data, three reduced scale prestressed concrete slabs supported on a spring subgrade and loaded through circular plates were tested to failure. Measurements of strain and deflection were made at a number of locations and load increments. Test variables included size of loading plate and magnitude of prestressing force.

Comparisons between test data and theory indicated fair agreement in values of deflection; however, measured strains were significantly smaller than predicted by theory. The theoretical assumption that the moment-curvature relationship can be represented by two straight lines—an elastic portion with a constant slope, followed by a plastic portion in which curvature may increase with no moment increase—is shown to be conservative for the static type of loading used. Under traffic load conditions, however, wherein a pattern of bottom surface cracks occurs, the theoretical moment-curvature assumption may be more closely approached. It is planned as part of the future testing program to investigate prestressed pavement response to repetitive moving loads.

•AN INTERIOR load of greater magnitude than one causing bottom surface cracking may be permitted on a prestressed concrete highway or airfield pavement. In the design of such pavements, it is therefore necessary to determine stresses and deflections for conditions not covered by the elastic theory. A theoretical procedure (1) was developed for this purpose at the PCA Research and Development Laboratories. This procedure is specifically applicable to a centrally loaded infinite slab supported by a "dense liquid" foundation and prestressed equally in longitudinal and transverse directions. It provides a method for predicting the distribution of moments and deflections in a prestressed concrete pavement for any load magnitude equal to or less than that causing top surface cracking if the radius of the loading plate, the cracking moment, the radius of relative stiffness, and the subgrade modulus are known. The location of

Paper sponsored by Committee on Rigid Pavement Design.

the top surface crack also can be estimated. In the development of this theoretical procedure, it was assumed that (a) the intensity of the subgrade reaction at each point of the bottom surface of the slab is proportional to the deflection of the slab at the point; (b) the moment-curvature graph is represented by two straight lines, i.e., an elastic portion with a constant slope, followed by a plastic portion in which curvature may increase with no moment increase; and (c) the radial cracks in the bottom surface of the concrete slab extend from the center of the load within a circular area that becomes larger as the load is increased. To determine the validity of these assumptions and to compare theoretical and measured data, a program of testing reduced scale precast prestressed concrete slabs was initiated.

OBJECTIVES AND SCOPE OF PROGRAM

The test program was designed to study the behavior of prestressed concrete slabs when subjected to interior loads sufficiently to cause both bottom and top surface cracking. While numerous variables deserve investigation, the reported tests are limited to slabs restrained to simulate infinite extent on a subgrade having an unvarying k value. Controlled variables included size of loading plate and magnitude of prestress.

The specific objectives of the program were (a) to compare measured deflected surface contours with theoretical values, (b) to compare stresses computed from measured strains with theoretical values, (c) to observe the manner in which bottom and top surface cracking occurred, and (d) to evaluate the assumptions made in developing the theoretical procedure.

TEST FACILITIES AND MATERIALS

Data are reported from load tests on three concrete slabs 8 ft by 8 ft by 1 in. thick. Prestressing was accomplished with pretensioned high-strength No. 12 steel wire. The slabs were precast, placed on an artificial coil spring subgrade, and load tested.

Prestressing

Uncoated stress-relieved steel wire was used for applying prestress at the mid-depth of the slabs. The wire diameter was 0.1055 in., area 0.00875 sq in., modulus of elasticity 27,600,000 psi, and ultimate strength 260,000 psi. The wire was tensioned in the frame shown in Figure 1. Two sides of the frame were formed by reinforced concrete beams anchored to the floor by post-tensioned steel bolts. Friction forces developed between the beams and the floor prevented movement due to tensioning of the wires. The wires were inserted through openings provided in these beams at 4-in. intervals along their lengths. The remaining two sides of the prestressing frame were formed by pairs of steel channels between which the wires were inserted. These channels reacted against the ends of the concrete beams.

Each prestressing wire was tensioned individually by a telescoping threaded spacer. The force in the wire was measured by a transducer (2) placed between the wire grip and the reaction frame at the side opposite the spacer. After tensioning the wires, a minimum of one day was allowed before casting the concrete slab. The force in each wire was checked and adjusted, if necessary, to the selected magnitude prior to casting.

To insure full prestress over as much of the slab as possible, a 1-in. split steel cube was fastened to each wire at the point where the wire entered the side forms. The two halves of the cube were grooved slightly undersize for the wire used and were clamped on the wire by countersunk machine screws.

Each slab was stressed equally in the longitudinal and transverse directions. The spacing between wires, amount of tensile force in each wire, and resultant concrete prestress are given in Table 1A.

Casting of Concrete

The cement factor of the concrete was 7.5 sk/cu yd; water-cement ratio was 0.45 by weight, and the sand-aggregate ratio was 0.59 by weight. Type 3 cement was used to obtain a high early strength, and the maximum size of gravel aggregate was $\frac{3}{8}$ in. The

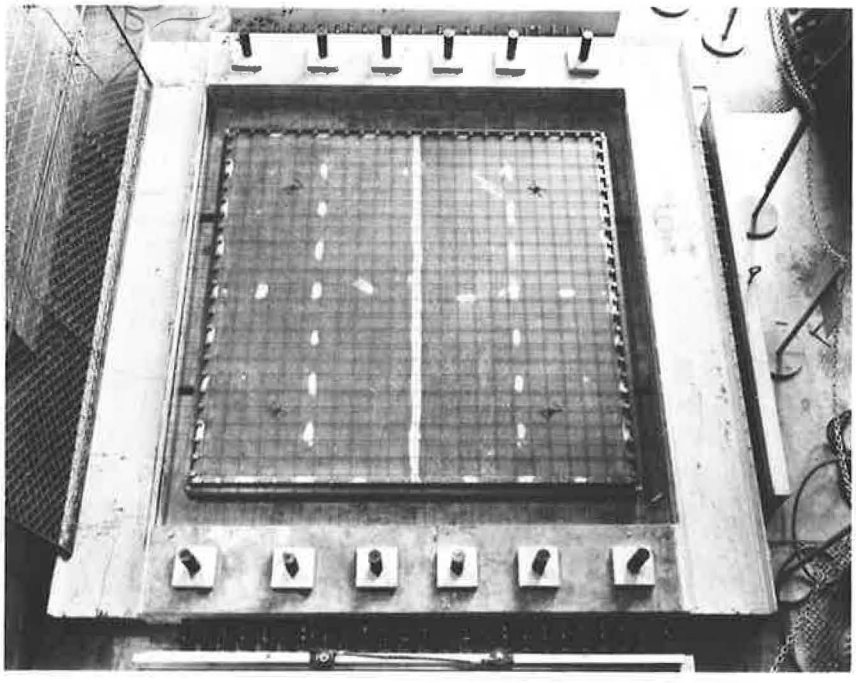

Figure 1. Casting bed.

slump averaged 4 in. and vinsol resin was added to provide an average air content of 5 percent.

Beams (6 by 6 by 30 in.) and cylinders (6 by 12 in.) were made at the time of casting. These were cured in a 70 F, 100 percent relative humidity room until the slabs were load tested, a period of from 8 to 10 days. As determined from tests on the beams and cylinders, the average compressive strength of the concrete was 5,770 psi, modulus of rupture 630 psi, and elastic modulus 3,500,000 psi.

After casting, each slab was covered with polyethylene sheeting and cured at a temperature of 70 to 75 F until the concrete had attained sufficient strength to permit release of the tension in the steel wires. Both top and bottom surfaces were then coated with a curing compound to reduce moisture losses and thereby minimize curling. Strain gages were then cemented to the slab surface at the desired locations.

Spring Subgrade

The artificial subgrade was composed of 121 coil springs, 5½-in. diameter and

TABLE 1

EXPERIMENTAL AND THEORETICAL DATA

A. Experimental Properties[a]

Slab No.	Wire Spacing (in.)	Wire Tensile Force (lb)	Concr. Prestr. (psi)	a (in.)	Mod. of Rupture (psi)	σ_c (psi)	m_c (in.-lb/in.)	L (in.)	α
1	4	1,200	300	3	630	930	155	9.54	0.315
2	4	1,200	300	5	630	930	155	9.54	0.525
3	4	600	150	3	630	780	130	9.54	0.315

[a]Symbols used are
a = radius of loading plate, in.;
σ_c = cracking stress = modulus of rupture plus prestress;
m_c = cracking moment $\sigma_c h^2/6$;
h = thickness of slab, 1 in.;
L = radius of relative stiffness $\sqrt[4]{\frac{E h^3}{12(1-\mu^2)k}}$;
E = elastic modulus, 3,500,000 psi;
μ = Poisson's ratio, assumed 0.15;
k = subgrade modulus, 36 pci; and
$\alpha = a/L$.

B. Experimental Values[b]

Slab No.	a (in.)	Prestress (psi)	Cracking Loads		b (in.)	c (in.)	Punching Failure Load (lb)
			Bottom (lb)	Top (lb)			
1	3	300	880	4,140	11½	14	9,000
2	5	300	1,220	4,820	11½	14	12,500
3	3	150	850	4,180	12¼	14	8,000

[b]Symbols used are
a = radius of loading plate, in.;
b = average distance bottom radial cracks extended from load center at top cracking load, in.; and
c = average radius of initial top circular crack, in.

C. Theoretical Values

Slab No.	Cracking Loads		Radius of Top Crack (in.)
	Bottom (lb)	Top (lb)	
1	900	2,950	8.5
2	1,270	3,570	11.5
3	780	2,470	8.5

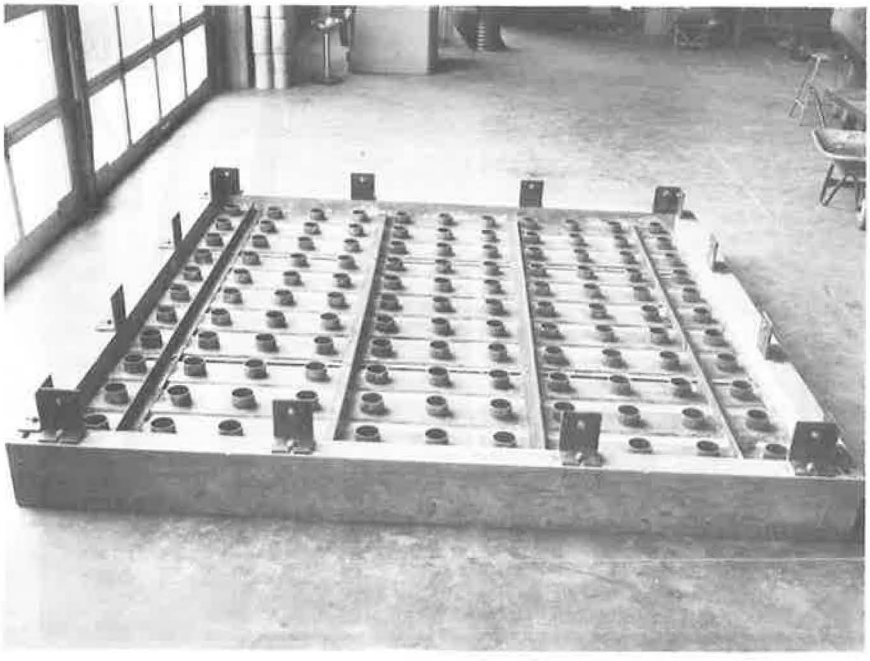

Figure 2. Concrete box before coil spring placement.

Figure 3. Concrete box with coil springs and top plates in place.

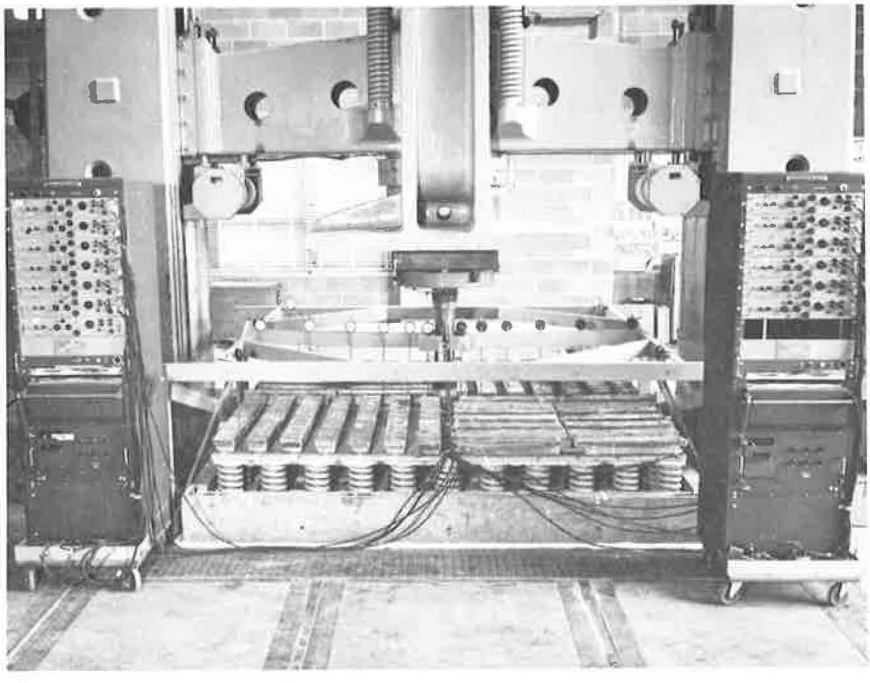

Figure 4. Load test on concrete slab.

8 in. long. Load-deflection tests conducted on eight randomly selected springs indicated that the spring constant was 2,915 lb per in. of deflection. The springs were placed at 9-in. centers in the concrete box shown in Figures 2 and 3. Short lengths of pipe connected to the bottom of the box positioned the springs and prevented lateral movement during load testing. Similar short lengths of pipe welded to 6-in.-square plates were placed in the top of each spring.

Prior to each slab test, a small quantity of mortar was placed between the polyethylene sheets on top of each spring plate; the slab was then lowered carefully into place compressing the mortar slightly and providing uniform contact over all springs. From the spring constant and spring spacing, the average subgrade modulus over the area of the slab was 36 pci.

Load Application

Loads were applied to the concrete slabs through centrally located circular plates of 3- or 5-in. radius (Table 1A). The concrete box holding the springs was designed to fit on the platen of a 1 million lb testing machine. A surcharge of lead weights, shown in Figure 4, totaling 6,400 lb was placed uniformly over the top surface of the slab to satisfy the requirements of model scaling and to permit the slab to act as an infinite plate.

INSTRUMENTATION

A typical instrumentation plan is shown in Figure 5. SR-4 type A9-2 strain gages 4 in. long were cemented to the top surface of each slab to measure the maximum compressive strain at the load and the distribution of radial and tangential strains at various distances from the load. Strains were recorded continuously throughout a load test.

The deflection pattern of each slab was determined by twenty-eight 0.001-in. dial indicators attached to a wooden bridge that rested on the machine platen. Deflection measurements were noted at each load increment.

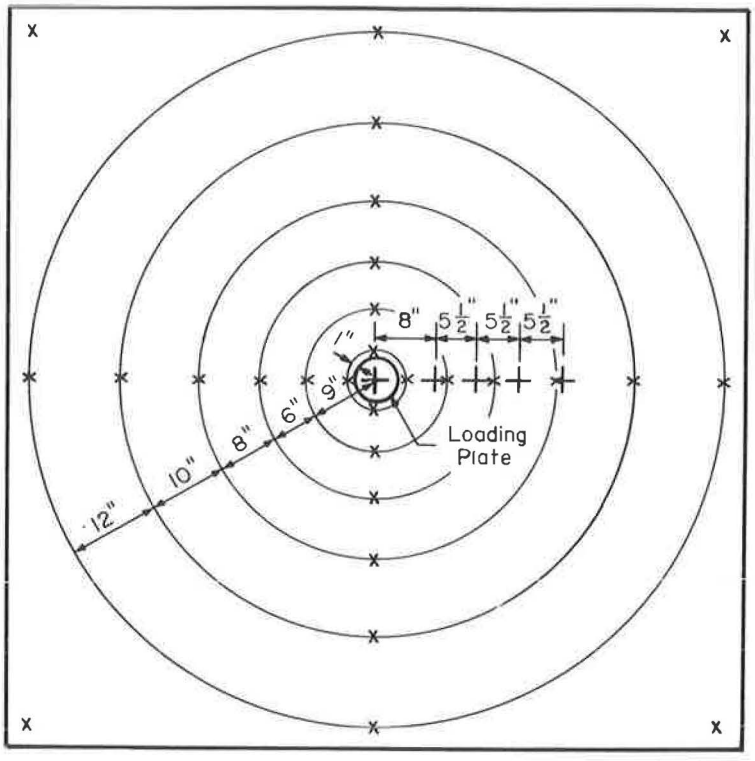

— Top Surface Strain Gage Location
X Deflection Dial Location

Figure 5. Typical instrumentation plan.

RESULTS

Load was increased in increments of 250 to 1,000 lb until the circular plate punched through the slab, failing the concrete in shear but leaving the prestressing wires intact. The punching failure loads were 9,000, 12,500, and 8,000 lb for Slabs 1, 2, and 3, respectively. Prior to punching failure, a number of concentric circular cracks were observed in the top surface. The initial top cracks were not visible until the load was about 7,000 lb; the radius was about 14 in. for all three slabs. After completion of test and release of load, the top cracks closed to such an extent that they were difficult to locate. A brittle coating of polyester resin applied in the later tests aided in locating cracks after release of load. A photograph of a top slab surface with the cracks outlined by black ink is shown in Figure 6. The bottom surface was also examined after completion of test. As shown in Figure 7, bottom cracks extended about 12 in. in radial directions from the load center.

Loads causing bottom and top surface cracking were those that produced tensile stresses at crack locations equal to cracking stresses. The cracking stress of each slab was assumed to equal the summation of the concrete modulus of rupture and the amount of prestress. As given in Table 1A, the cracking stress was 930 psi for Slabs 1 and 2 and 780 psi for Slab 3. Stresses in a radial and tangential direction computed from the measured strains by Eqs. 1 and 2 are shown in Figure 8.

$$\sigma_r = \frac{E}{1 - \mu^2} (e_r + \mu e_t) \qquad (1)$$

Figure 6. Top surface cracking after test of Slab 2.

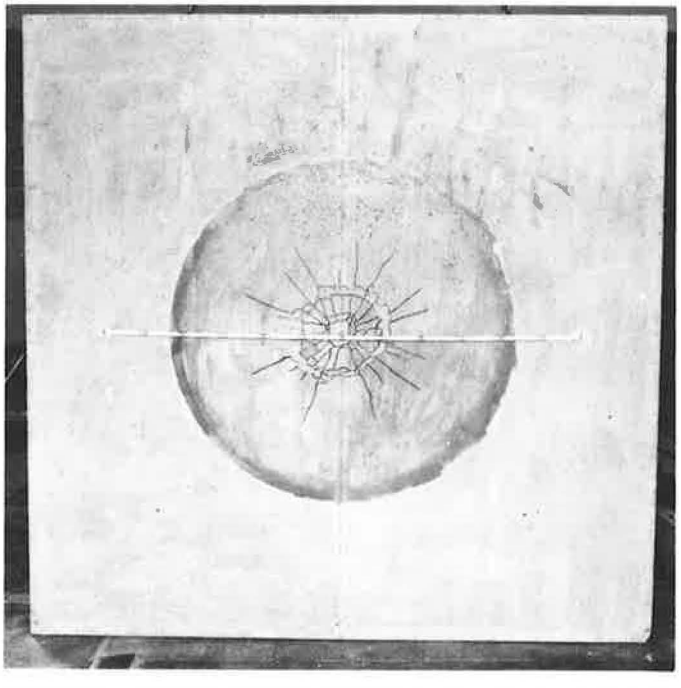

Figure 7. Bottom surface cracking after test of Slab 2.

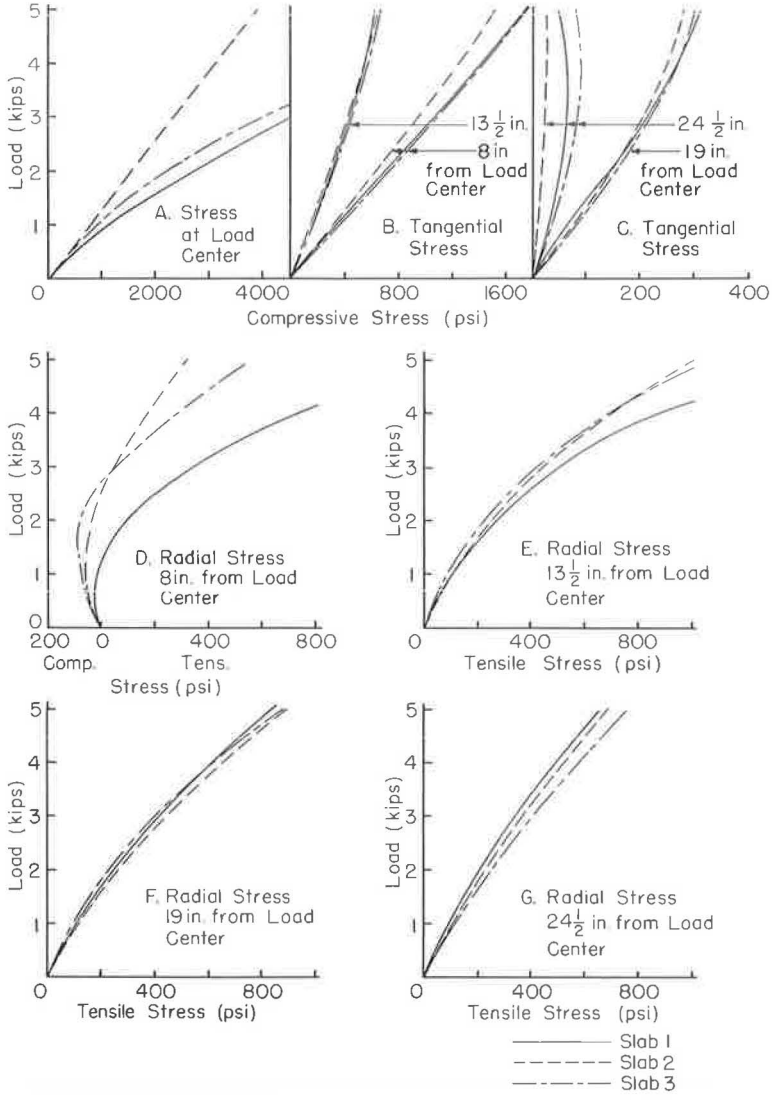

Figure 8. Top surface stresses.

$$\sigma t = \frac{E}{1 - \mu^2} (et + \mu e_r) \qquad (2)$$

in which

σ_r = radial stress,
σt = tangential stress,
e_r = measured radial strain,
e_t = measured tangential strain,
E = concrete modulus of elasticity, 3,500,000 psi, and
μ = Poisson's ratio, assumed 0.15.

Assuming the neutral axis to be at the mid-depth of the slab, top surface compressive stresses at the load center (Fig. 8A) were used to determine bottom surface crack-

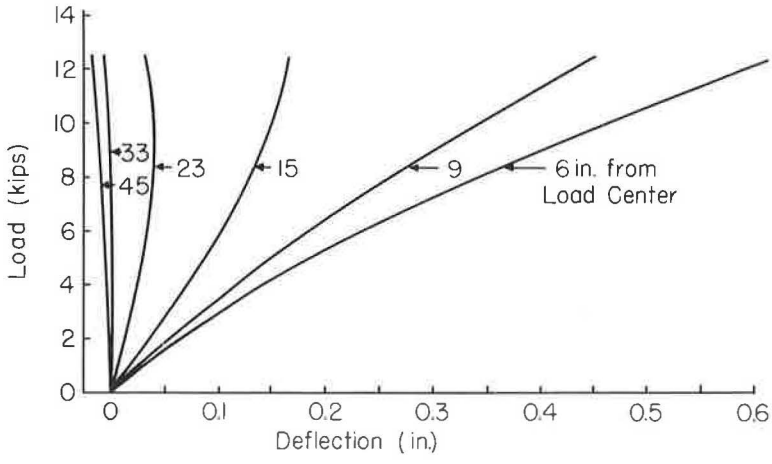

Figure 9. Deflection of Slab 2.

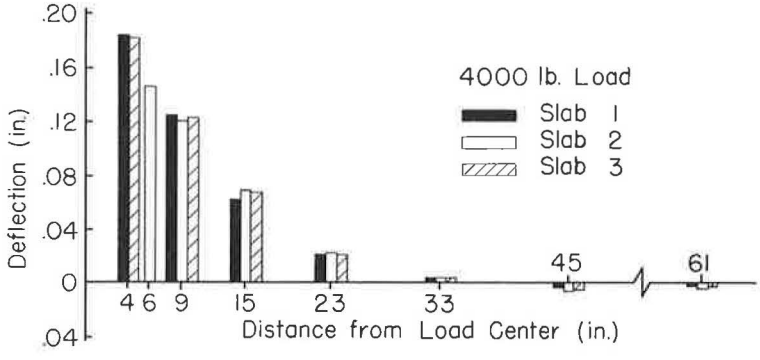

Figure 10. Comparison of slab deflections.

ing loads. Top surface radial tensile stresses 13½ in. from the load center (Fig. 8E) were used to determine top surface cracking loads. Bottom and top surface cracking loads computed from these stress diagrams are given in Table 1B.

Cracking loads were compared to determine the influence of prestress and loading plate size. Slab 2 with the same prestress as Slab 1 was loaded with a larger plate and had greater cracking loads. Slab 3 with less prestress than Slab 1 was loaded with the same plate size and had nearly the same cracking loads. Therefore, the test slab cracking loads were influenced more by loading plate size variations than by the difference in prestress.

The extended distance of bottom surface radial cracks from the load center were estimated by determining where the tangential stresses (Figs. 8B and 8C) exceeded the cracking stresses. Table 1B lists these distances, b, for the load that produced top surface cracking. This distance was slightly greater for Slab 3, which had the smallest amount of prestress.

Deflections were measured incrementally at seven different distances from the load center with a total of 28 indicators as shown in Figure 5. At each distance from the load center, the four indicators spaced 90° apart provided similar deflections at each load increment throughout a test. This indicated that the pressure under the load plate was symmetrically distributed and that the coil spring subgrade responded properly.

Average deflections measured during the load test of Slab 2 are shown in Figure 9. These are typical of all three slabs. There was no abrupt change in the rate of deflec-

tion increase per unit load when either bottom or top surface cracking occurred. A comparison between deflections for the three slabs at a load of 4,000 lb is shown in Figure 10. This load approaches the magnitude causing top surface cracking. Deflections of the three slabs were similar, indicating only minor influence of variations in prestress and size of loading plate.

THEORETICAL VALUES

Experimental data were compared with values determined by the theoretical procedure (1) developed at the PCA Research and Development Laboratories for a centrally loaded infinite slab supported by a "dense liquid" foundation and prestressed equally in longitudinal and transverse directions. The explicit parameters necessary for the computation of theoretical values are cracking moment, subgrade modulus, and the ratio of

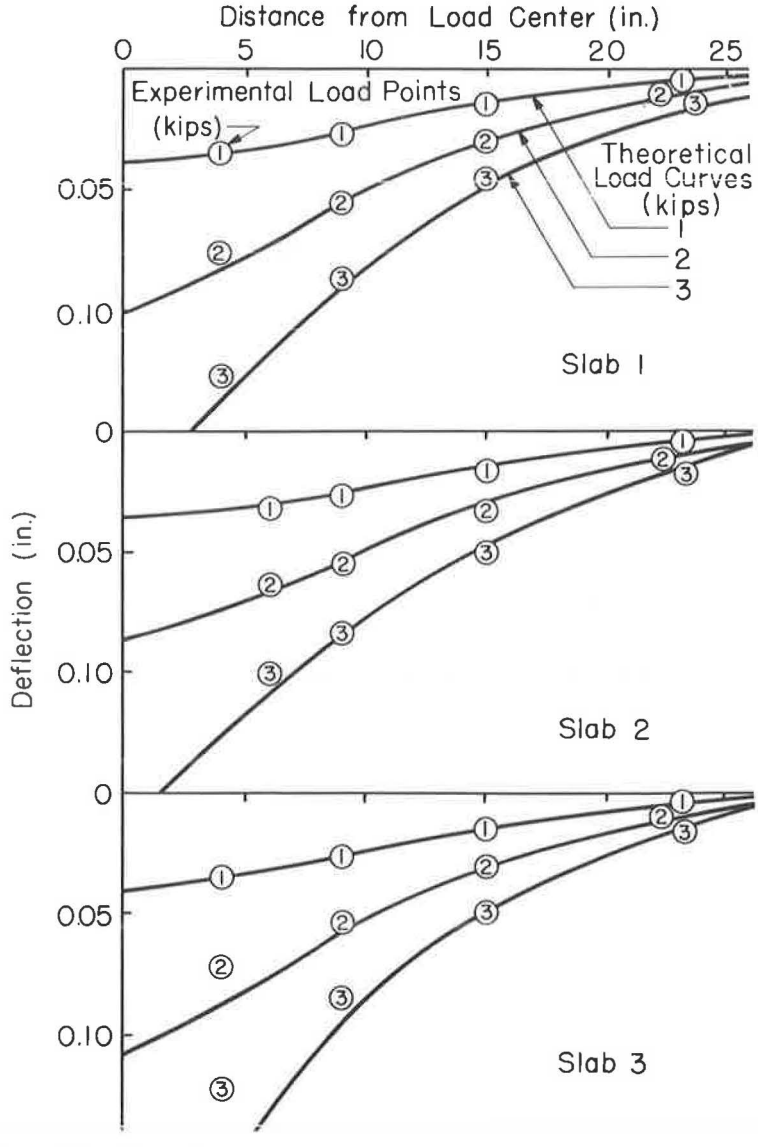

Figure 11. Comparison of experimental and theoretical deflections.

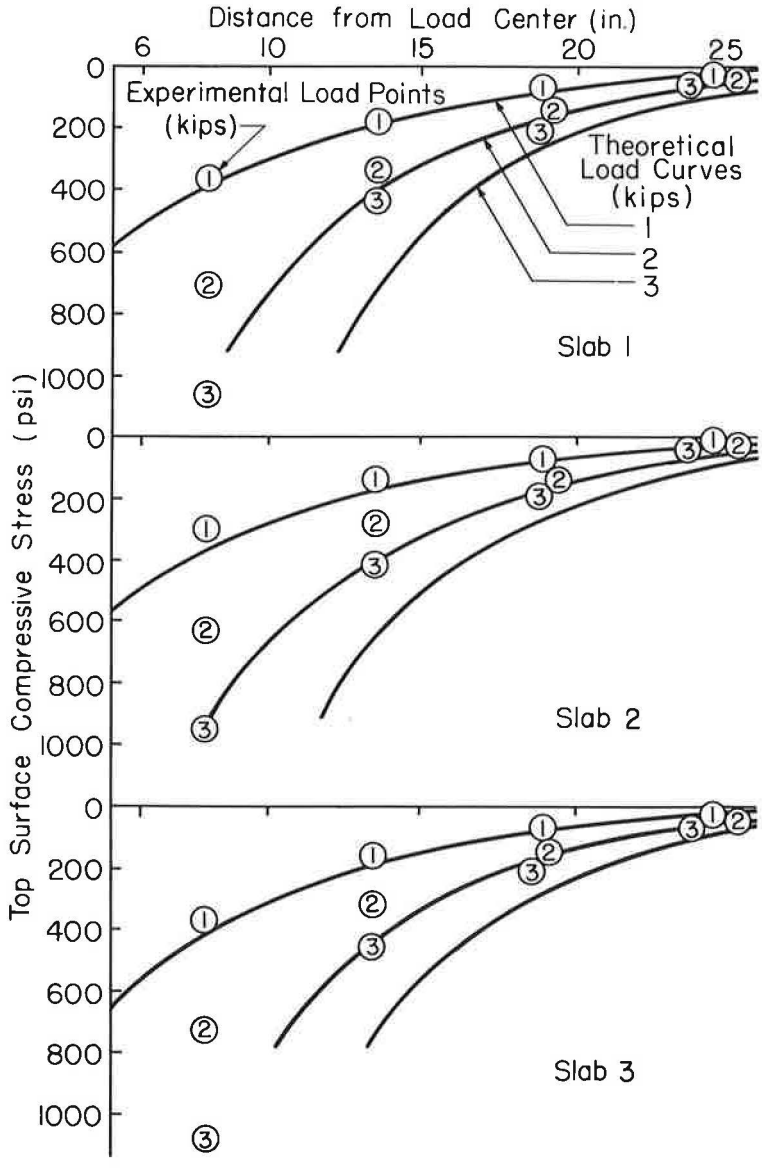

Figure 12. Comparison of experimental and theoretical tangential stresses.

the radius of the loading plate to the radius of relative stiffness. These quantities for the three slabs are given in Table 1A.

Theoretical deflection, tangential stress, and radial stress are shown by the curves in Figures 11, 12, and 13, respectively, for load applications of 1,000, 2,000, and 3,000 lb on each slab. The numbered circles are experimental results. The influence that prestress and loaded area size have on stresses and deflections predicted by the theoretical procedure was determined from these figures. Slab 2 had the same prestress as Slab 1 but was loaded with a larger plate. Slab 3 was loaded with the same plate size as Slab 1 but had less prestress. According to the theoretical treatment, increased deflections, tangential stresses, and radial stresses should result from a decrease in either the prestress or loaded area size. Experimental tangential stresses

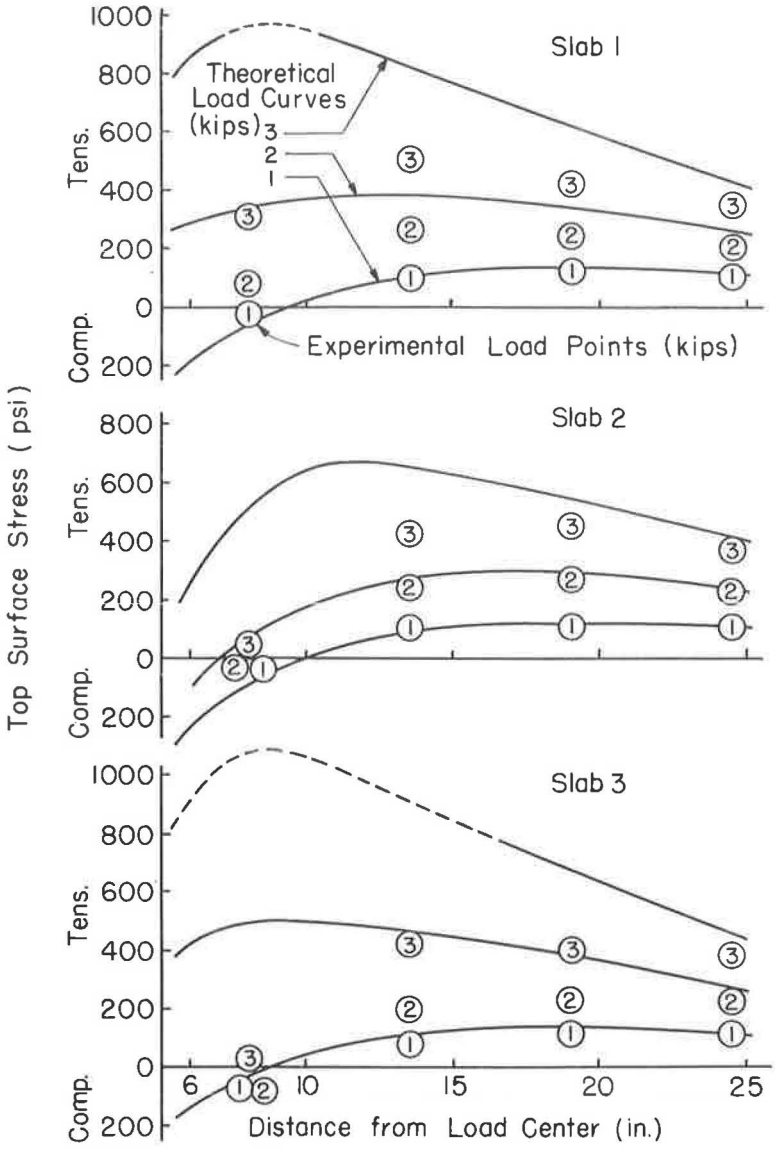

Figure 13. Comparison of experimental and theoretical radial stresses.

were influenced in this manner with Slab 3 showing the largest values and Slab 2 the smallest values. However, experimental deflections and radial stresses varied only slightly with changes in prestress and loaded area size.

Good agreement was found between experimental and theoretical data for the 1,000-lb load. At greater loads, the experimental deflections were in fair agreement with the theoretical values, but the experimental stresses especially those in the radial direction were smaller than the theoretical values. As a result of the radial stress differences, the experimental and theoretical loads for top cracking differed considerably.

Theoretical cracking loads and radii of top circular cracks are given in Table 1C. A comparison with Table 1B indicates that experimental and theoretical bottom cracking loads were in excellent agreement but that experimental top cracking loads and

radii of top circular cracks were greater than the theoretical values. Theoretical bottom cracking loads were computed by methods based on the elastic theory, and their agreement with experimental values indicated elastic slab behavior prior to cracking. Reasons for the disparity beyond elastic conditions were investigated.

A possible discrepancy between theory and experiment could result from the manner in which the load was distributed between the load plate and the test slab. Although a ½-in. rubber pad was placed between the steel plate and concrete slab to aid in obtaining uniform load distribution, at higher magnitudes of load the combination of large slab deflections and a relatively stiff loading plate might have concentrated the load around the periphery of the plate.

Stresses at locations beyond the loading plate area resulting from a peripheral concentration of load would theoretically be equivalent to those resulting from a uniform load distributed through a plate having a radius of about 1.5 times as large. To explore this conjecture, the experimental values of Slab 1 were compared with theoretical values determined for a uniformly loaded plate of 4½-in. radius. As shown by the tangential and radial stresses in Figure 14, there was better agreement between experimental and theoretical values for the peripheral loading condition than for the uniformly loaded 3-in. radius plate conditon shown in Figures 12 and 13. However, the differences between experimental and theoretical stresses remained greater than magnitudes that might be attributed to test conditions. Therefore, the assumptions used in the development of the theoretical procedure were examined to obtain an explanation for the differences.

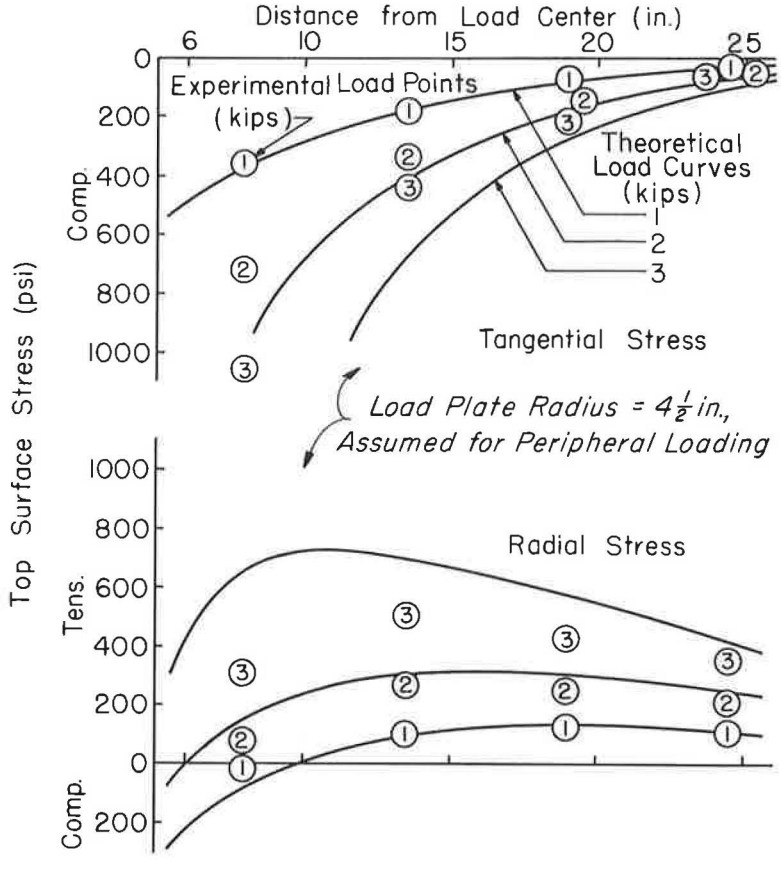

Figure 14. Comparison of experimental and theoretical stresses of Slab 1.

Three assumptions were involved: (a) that the intensity of subgrade reaction at each point of the bottom surface of the slab was proportional to the deflection of the slab at that point; (b) that the radial cracks in the bottom surface of the concrete slab extended from the center of the load within a circular area that became larger as the load was increased (Fig. 15A); and (c) that the relationship between moment and curvature was represented by two straight lines (Fig. 15B), that is, an elastic portion with a constant slope followed by a plastic portion in which curvature increased with no moment increase. The first assumption was fulfilled by the use of a coil spring subgrade, and the

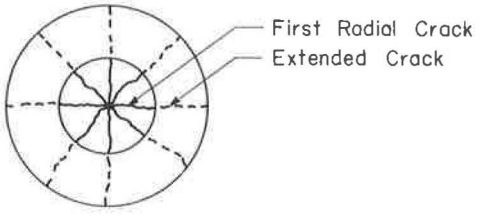

A. Assumed Bottom Surface Crack Pattern

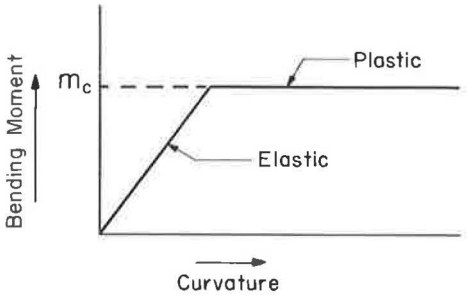

B. Assumed Moment-Curvature Relationship

Figure 15. Theoretical assumptions.

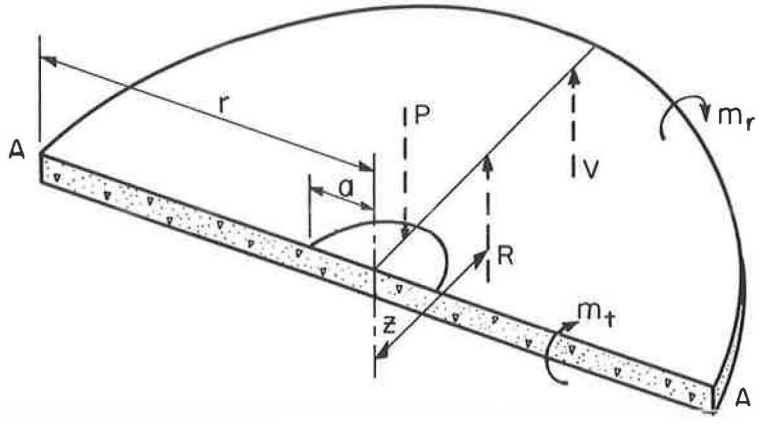

Figure 16. Semicircular portion of concrete slab with interior load.

second assumption was confirmed by the experimental data. To determine the accuracy of the third assumption, the following analysis of a free-body diagram of a loaded slab was undertaken.

The analysis was developed for a large concrete slab loaded at an interior location with a force of 2P uniformly distributed over a circular area of radius a. A semicircular section of this slab including half the loaded area is shown in Figure 16. The resultant applied load on this section is labeled P, the resultant subgrade reaction R, and the resultant shear force V. The moments consist of the radial moment per unit length, m_r, and the tangential moment per unit length, m_t. The shear and radial moments were assumed to be uniformly distributed along the circular arc of radius r measured from the center of the load.

Moments were summed about diameter A-A. The moment arm of the resultant applied load P is equal to $4a/3\pi$ assuming uniform distribution of load over the semicircular area of radius a. The moment arm of the resultant shear force V is equal to $2r/\pi$ assuming uniform distribution along the circular arc of radius r. The moment about A-A of the unit radial moment, m_r, is $2r\, m_r$. The average unit tangential moment along the diameter 2r is $\overline{m}_t$, and its moment about A-A is $2r\, \overline{m}_t$. The sum of moments about diameter A-A must equal zero as shown by Eq. 3.

$$\Sigma M_{AA} = O = P\left(\frac{4a}{3\pi}\right) - Rz - V\left(\frac{2r}{\pi}\right) + 2r\,(m_r + \overline{m}_t) \qquad (3)$$

The resultant subgrade reaction R can be computed for any semicircular section of radius r by multiplying the displaced volume as determined from the measured deflections by the known subgrade modulus. Its moment arm z can be computed by locating the centroid of the displaced volume. The difference between the load and subgrade reaction forces is equal to the resultant shear force. Therefore, diagrams of $\overline{m}_t + m_r$ vs r can be determined for each increment of load applied to a test slab by using the measured deflection profile and the subgrade modulus.

The accuracy of the moment-curvature relationship assumed in the theoretical procedure was determined by the combined use of $\overline{m}_t + m_r$ diagrams and measured strain data. An example of the method employed before the occurrence of bottom surface cracking is given in Figure 17 using the data obtained when a 500-lb load was applied to Slab 1. As shown in Figure 17A, the deflection profile was obtained by drawing a smooth curve through the measured experimental values. This profile was used with the analysis outlined in the previous paragraph to obtain the $\overline{m}_t + m_r$ diagram shown in Figure 17B. As the slab reacted elastically before the occurrence of bottom cracking, the ratio of a $\overline{m}_t + m_r$ diagram to a $(\overline{\sigma}_t + \sigma_r)/E$ diagram was equal to the elastic modulus multiplied by the unit section modulus. Using the elastic modulus of 3,500,000 psi that was determined from beam and cylinder test specimens and 1/6 for the unit section modulus, the curve in Figure 17C was obtained from Figure 17B. Profiles of σ_t/E and σ_r/E were also obtained (Fig. 17D) by drawing smooth curves through values computed from the measured strains by Eqs. 1 and 2 rewritten to give σ_r/E and σ_t/E in terms of the strains. The σ_t/E profile was used to compute a profile of cumulative average tangential stress divided by elastic modulus or $\overline{\sigma}_t/E$. For this computation, average values for 2-in. increments were summed and divided by the number of increments. Differences between the σ_r/E and $\overline{\sigma}_t/E$ profiles in Figure 17D at locations of computed experimental values are represented by the points shown in Figure 17C. There was good agreement in Figure 17C between the points determined from the strain data and the curve determined from the deflection data using the elastic modulus of 3,500,000 psi from beam and cylinder tests. As similar good agreement was obtained for Slabs 2 and 3, the experimental data and method of analysis were considered to be reliable.

An example of the method employed after the occurrence of bottom surface cracking is shown in Figure 18 using the data obtained when a 3,000-lb load was applied to Slab 1. The $\overline{m}_t + m_r$ diagram computed with the use of the deflection profile is shown by curve A. Radial strains measured at distances of 8, 13½, 19, and 24½ in. from the load center were used to compute radial stresses. These stresses, which were less than the cracking stresses, were multiplied by the unit section modulus to obtain unit

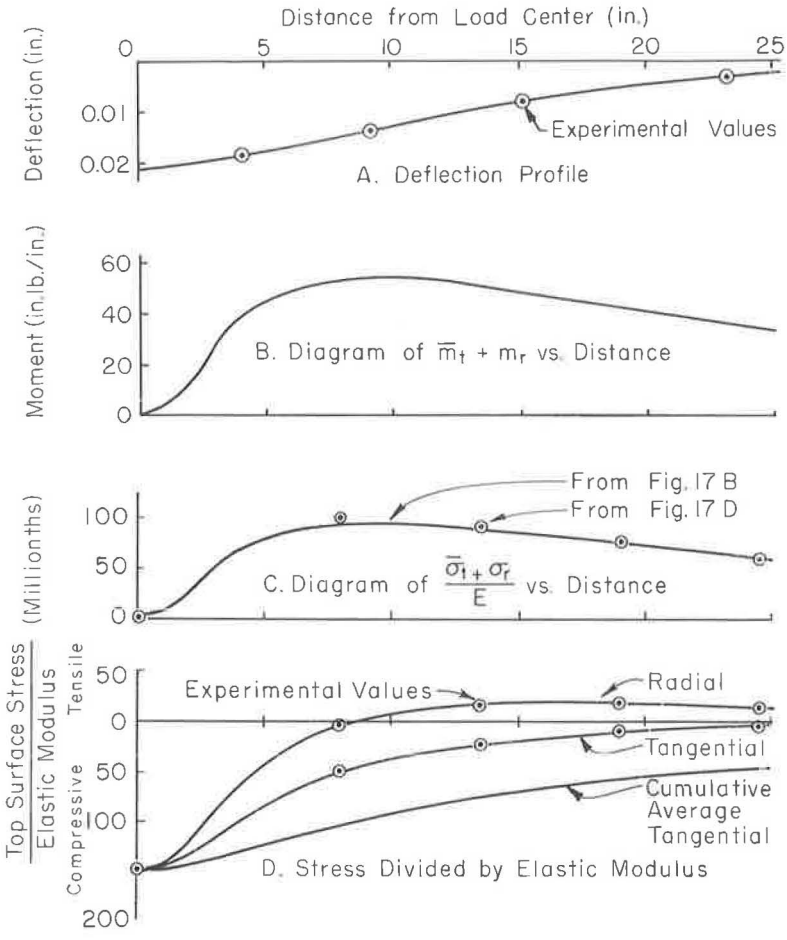

Figure 17. Diagrams for 500-lb load on Slab 1.

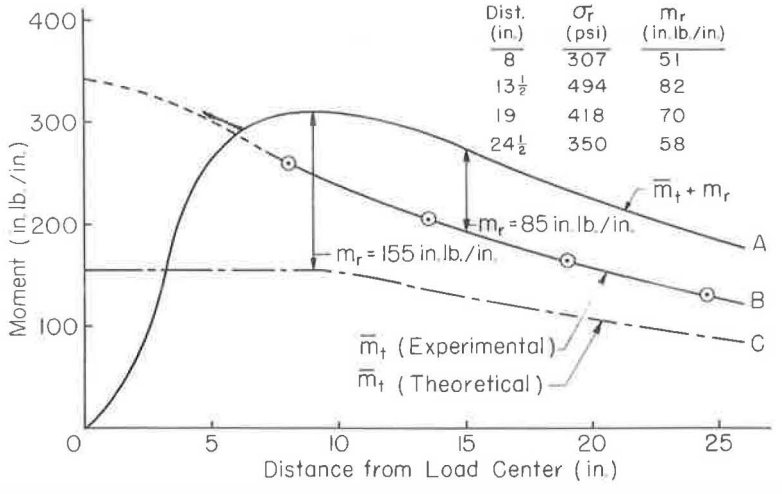

Figure 18. Moment diagrams for 3,000-lb load on Slab 1.

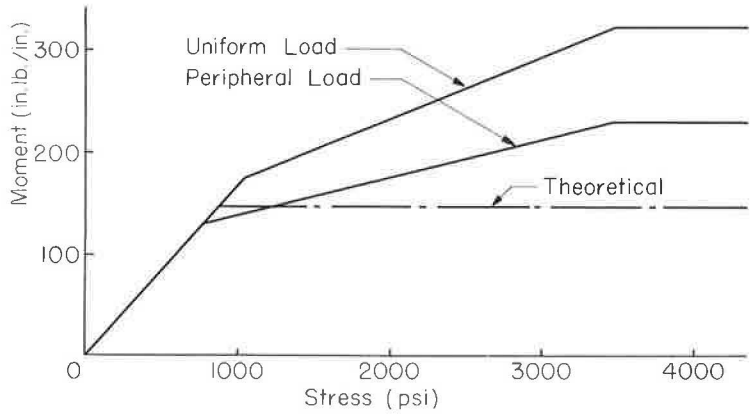

Figure 19. Moment-stress diagrams.

radial moments. These unit radial moments, m_r, were subtracted from the $\overline{m}_t + m_r$ diagram shown by curve A to obtain the average unit tangential moment, $\overline{m}_t$, diagram shown by curve B.

The cracking moment of Slab 1 was 155 in. lb/in. If the loaded slab had reacted according to the moment-curvature assumption used in the theoretical method, the maximum unit tangential moment would equal the cracking moment and the $\overline{m}_t$ diagram would be as represented by curve C. A comparison of the experimental and theoretical $\overline{m}_t$ diagrams indicated that tangential moments greater than those causing initial cracking occurred in the test slabs.

The example in Figure 18 was used to demonstrate that the occurrence of moments greater than those causing initial cracking was the major reason for differences between experimental and theoretical data. The maximum negative radial moment determined from the difference between curves A and B occurred 15 in. from the load center and equaled 85 in. lb/in. or 55 percent of the cracking moment of 155 in. lb/in. These values were for a load of 3,000 lb. Top surface cracking occurred at 4,140 lb with a radius of 14 in. as given in Table 1B. The maximum negative radial moment determined from curves A and C occurred 9 in. from the load center and equaled the cracking moment of 155 in. lb/in. at this 3,000-lb load. As given in Table 1C, the theoretical procedure predicted top surface cracking at 2,950 lb with a radius of 8.5 in. Therefore, the test slabs would have cracked approximately as predicted by the theoretical procedure if they had reacted in accordance with the theoretical moment-curvature assumption.

Average unit tangential moment, $\overline{m}_t$, diagrams obtained as shown by the example in Figure 18 were used to compute unit tangential moment, m_t, diagrams. By comparing m_t diagrams with tangential stress profiles determined from experimental strain data, moment-stress diagrams were obtained. The moment-stress diagrams (Fig. 19) were composed of the three connecting straight lines that provided the best agreement between moment and stress profiles of the three slabs for all loads less than those causing top surface cracking. A moment-stress diagram was determined for both the uniformly loaded area condition and the peripheral load condition previously described. Both diagrams were determined by the same procedure except that the moment arm of the resultant applied load as given in Eq. 3 was $2a/\pi$ for the peripheral load condition instead of $4a/3\pi$ as used for the uniformly loaded area. The moment-stress diagram resulting from the moment-curvature assumption of the theoretical procedure is also shown in Figure 19. A comparison of these diagrams indicates again that moments greater than the initial cracking moments occurred in the test slabs. Therefore, the slabs did not react in accordance with the assumption that the moment-curvature relationship can be represented by two straight lines with the maximum moment equaling the cracking moment.

CONCLUSIONS

Three reduced scale prestressed concrete slabs supported on a coil spring subgrade were loaded to failure through centrally located circular plates. Measurements of strain and deflection were made at a number of locations with a number of load increments. Test variables included loading plate size and prestressing force magnitude. The following conclusions were drawn:

1. Initial slab cracking occurred in the bottom surface under the loaded area. As the load was further increased, the bottom cracks extended in radial directions. At load averaging 4.4 times the bottom cracking load, a circular top surface crack occurred with a radius of 1.5 times the radius of relative stiffness. At load averaging 10.0 times the bottom cracking load, the loading plate punched through the slab failing the concrete in shear but leaving the prestressing wires intact. An increase in the size of loaded area caused an increase in the cracking loads. Additional prestress had little influence on the cracking loads.
2. A comparison between experimental data and values determined by a theoretical procedure developed at the PCA Research and Development Laboratories indicated the following: (a) experimental and theoretical bottom surface cracking loads were in excellent agreement; experimental deflection and stress profiles at bottom cracking loads were similar to theoretical profiles; (b) experimental top surface cracking loads were about 48 percent greater than theoretical values; at the top cracking loads, the experimental and theoretical deflections were in fair agreement, but the experimental stresses especially those in a radial direction were less than the theoretical values; and (c) observed radii of top surface circular cracks were greater than predicted by the theory.
3. An analysis of a free-body diagram of a loaded test slab indicated that moments greater than the initial cracking moment occurred after bottom surface cracking. Therefore, the slabs did not react in accordance with the assumption made in the theoretical procedure that the moment-curvature relationship can be represented by two straight lines with the maximum moment equaling the cracking moment. This was the major reason for greater experimental top cracking loads than theoretically predicted. The theoretical moment-curvature assumption is therefore conservative for static type loading. Under traffic load conditions, however, wherein numerous bottom surface cracks occur, the theoretical assumption may be more closely approached.

REFERENCES

1. Osawa, Y., "Strength of Prestressed Concrete Pavements." Jour. of the Structural Div., ASCE Proc., PCA Dev. Dept. Bull. D57 (Oct. 1, 1962).
2. Hanson, N. W., "Load Cells for Structural Testing." Jour. of the PCA Res. and Dev. Labs., PCA Dev. Dept. Bull. D33 (Jan. 1959).